## 4.5 Reinforced Concrete Columns with Enhanced Ductility

### 1) Interlocking columns with large cross sections

Interlocking columns have been extensively implemented in New Zealand, USA and other countries (Park 1996, Priestley, Seible and Calvi 1996, Roberts 1999, Tanaka and Park 1993). The interlocking spirals provide confinement to enhance ductility of reinforced concrete columns. Prior to the 1995 Kobe earthquake, spirals were not used because rectangular columns were generally preferred and because column diameters are generally larger. Since the 1995 Kobe earthquake, the interlocking spiral columns have been recommended in the design codes (JRA 1996), and various studies have been conducted (Fujikura et al 2000, Shito et al 2002, Yagisita, Tanaka and Park, 1997).

Interlocking spiral columns with large sections were constructed at Kamanashi bridge as shown in Photo 4.1. Each column consists of 2 spirals with a diameter of 6 m and is 8.5 m wide and 6 m long in the transverse and the longitudinal directions, respectively. Since these columns were much larger in size than the interlocking columns which have been constructed elsewhere, a unique experimental test was conducted by the Japan Highway Public Corporation (JH) in conjunction with the construction of the bridge. Since assemblage of the interlocking spirals requires special skill, an onsite assemblage test of large diameter interlocking spirals was conducted (Shito et al 2002).

In the cyclic loading test, several model columns with interlocking spirals were loaded independently in the transverse and the longitudinal directions. The model columns were 2.7 m tall (effective column height) and 900 mm wide and 600 mm long in the transverse and longitudinal directions, respectively. They consisted of two spirals with a diameter of 600 mm. They were about 1/10 geometrically scaled models. The concrete strength was 28.1-39.7 MPa. The volumetric tie reinforcement ratio was 0.19%, 0.29% and 0.52% with the longitudinal reinforcement ratio being 1.63%. A 900 mm wide and 600 mm long standard rectangular column was also constructed for comparison. In addition to ties, cross ties were laterally spaced at every 158-196 mm interval in the standard rectangular column. The concrete strength of the rectangular column was 39.8 MPa. The longitudinal reinforcement ratio was 1.18% and the volumetric tie reinforcement ratio including the cross ties was 0.88%.

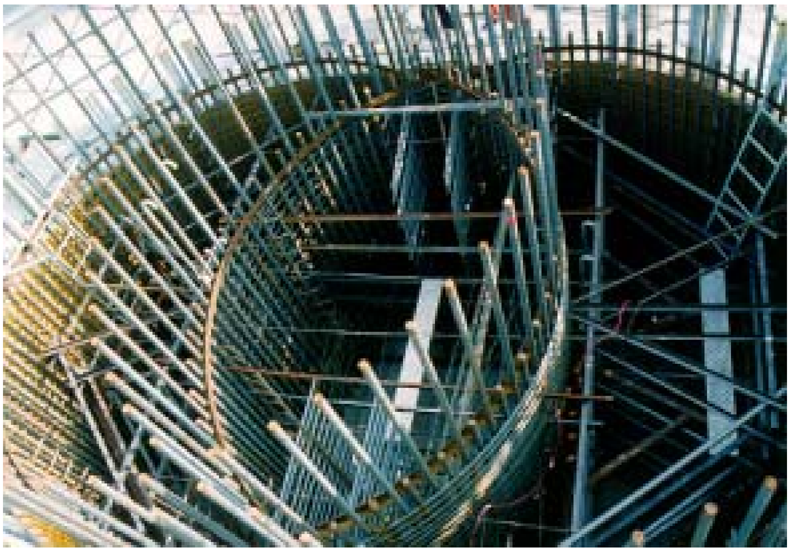

Photo 4.1 Construction of 8.5 m Wide and 6 m Long Interlocking Spiral Column (Shito et al 2002)

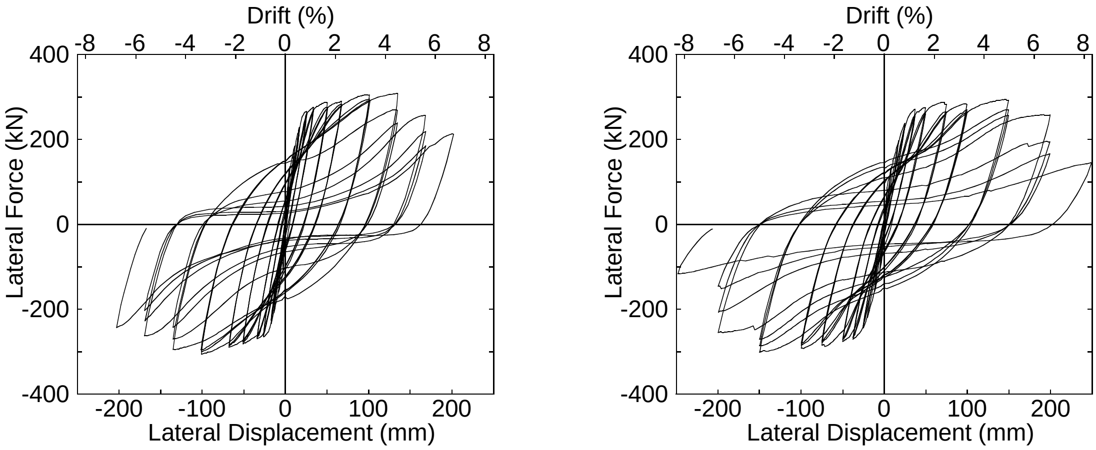


(a) Standard Columns

(b) Interlocking Spiral Columns with Volumetric Ratio of 0.29%

Fig.4.48 Effect of Interlocking Spirals (Shito et al 2002)

Photo 4.2 Assembling of Spirals (Shito et al 2002)

Fig. 4.48 compares the lateral force vs. lateral displacement hystereses of the interlocking spiral column (volumetric tie reinforcement ratio is equal to 0.29%) and the standard rectangular column under a cyclic loading in the longitudinal direction. The lateral restoring force is stable until 4.5% drift in the rectangular column, while it is stable until 5% drift in the interlocking spiral column. A similar test was conducted to verify that the interlocking columns exhibit stable hysteresis under a cyclic loading in the transverse direction.

Since the diameter of the interlocking spirals is large at Kamanashi bridge, an onsite assemblage test of the interlocking spirals was conducted, as shown in Photo 4.2, using a 4.5 m wide and 3 m long column consisting of two interlocking spirals with a diameter of 3 m. Two spirals were interlocked after being hung separately using a balanced lever, and they were set in position from the top of longitudinal bars. The spirals were temporally fixed to hanging cables so that they were set with an expected vertical interval. This construction procedure was successfully implemented on the interlocking column shown in Photo 4.1.

**2) Unbonding of longitudinal bars at the plastic hinge**

In a reinforced concrete column, the longitudinal bars damage progresses from local buckling to rupture in the plastic hinge under an extreme earthquake excitation. The bond between the longitudinal bars and the concrete results in the concentration of damage to the longitudinal bars at a specific localized interval where the local buckling occurs at the first time.

One of the measures used to mitigate such concentrated damage to the longitudinal bars is to unbond the longitudinal bars from the concrete at the plastic hinge (Takiguchi, Okada and Sakai 1976). By appropriately unbonding the longitudinal bars between an interval with length $L_{ub}$ as shown in Fig. 4.49, the deformation of the longitudinal bars is reduced by

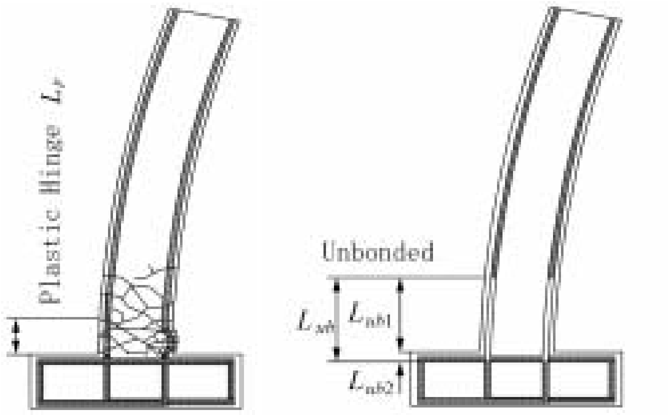


(a) Standard Column (b) Unbonded Column

Fig.4.49 Unbonding of Longitudinal Bars

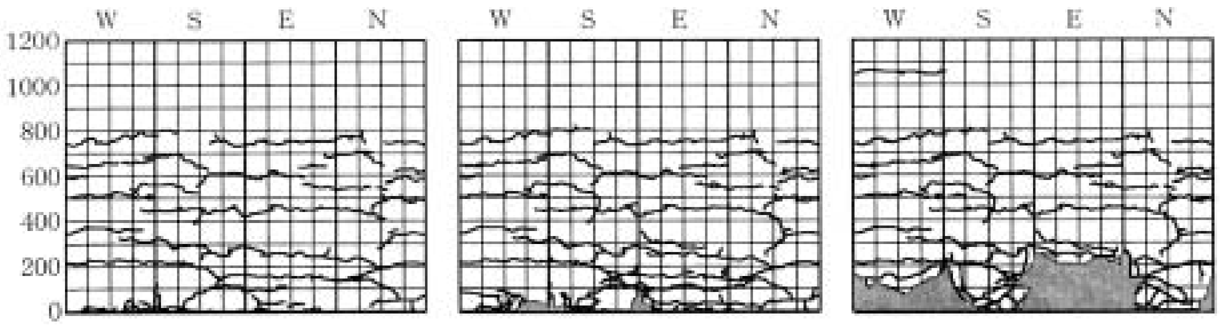


(a) $5\delta_y$ ( =2.2% drift ) (b) $8\delta_y$ ( =3.5% drift ) (c) $11\delta_y$ ( =4.8% drift )

(1) Standard Column

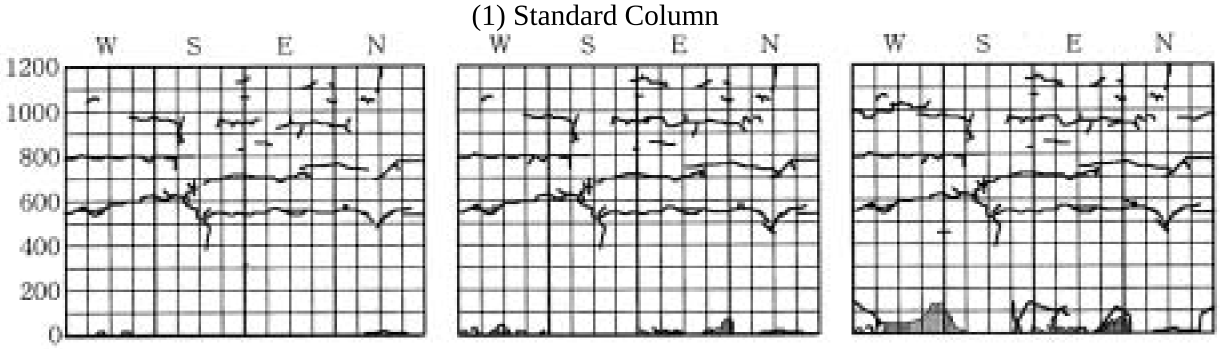


(a) $5\delta_y$ ( =2.2% drift ) (b) $8\delta_y$ ( =3.5% drift ) (c) $11\delta_y$ ( =4.8% drift )

(2) Unbonded Column ( Loaded in EW Direction )

Fig.4.50 Progress of Damage

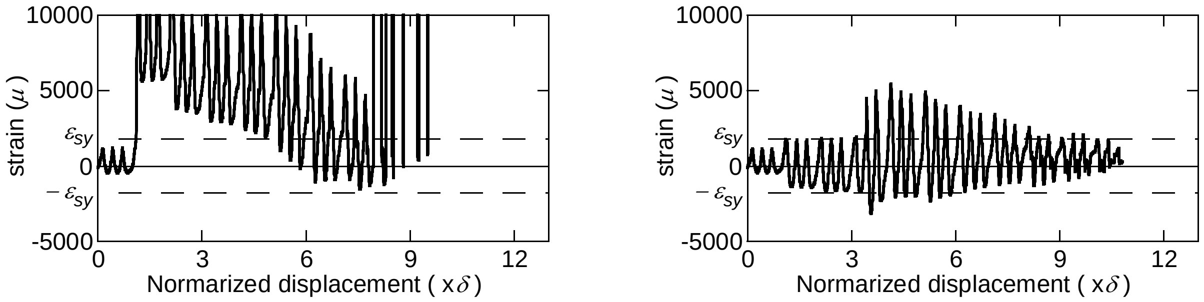


(a) 25mm from the base (b) 175mm from the base

(1) Standard Column

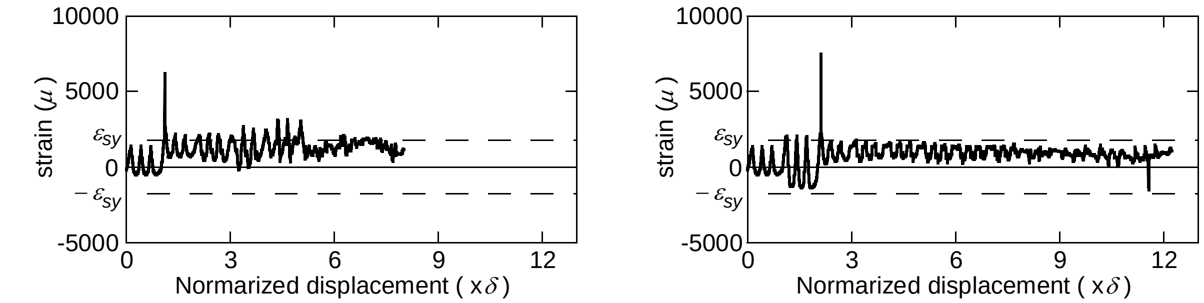


(a) 25mm from the base (b) 175mm from the base

(2) Unbonded Column

Fig.4.51 Strain on a Longitudinal Bar

avoiding the concentration of strain as a result of averaging the strain in the interval $L_{ub}$. The unbonding may be achieved by wrapping the longitudinal bars with plastic materials. Protection may be required for corrosion of the unbonded longitudinal bars.

Fig. 4.50 shows the effect of unbonding the longitudinal bars in a 1.45 m tall square column with a width $D$ equal to 400 mm (Kawashima, Hosoiri, Shoji and Sakai 2001). Although several tests were conducted, only two cases are presented here. The concrete strength is 24 MPa. The longitudinal reinforcement ratio is 0.95%, and the volumetric tie reinforcement ratio is 0.77%. The longitudinal bars are unbonded for a length of the column width $D$. In the standard column, the covering concrete starts to significantly spall off at $8\delta_y$, in which $\delta_y$ is the yield displacement of the standard column. Since $\delta_y$ is equal to 6 mm, 1% drift corresponds to $2.3\delta_y$. The column was cyclically loaded 3 times at each loading displacement $\delta_y$, $2\delta_y$, $3\delta_y$, …., until failure. The same loading hysteresis was used for both the standard and the unbonded columns.

The concrete failed within about 200 mm from the bottom after $11\delta_y$ (=4.8% drift) in the standard column. In comparison, the failure of concrete is much less in the unbonded column than the standard column. The covering concrete failed no higher than120 mm from the bottom even after $13\delta_y$ (=5.7% drift). Fig. 4.51 compares the strains on a longitudinal bar at 25 mm and 175 mm from the bottom of the column. The strain at 25 mm builds up over the yield strain at the first load excursion of $2\delta_y$. On the other hand, the strain on a longitudinal bar that is unbonded for a length of $D$ is much smaller than the strain on a longitudinal bar in the standard column. The strains are similar, although not the same, at 25 mm and 175 mm from the bottom in the longitudinal bar in the unbonded column. The strains on the longitudinal bars become larger than 6,000 $\mu$ at 25 mm and 175 mm from the bottom at the first excursion of $2\delta_y$ and $3\delta_y$ loadings, respectively.

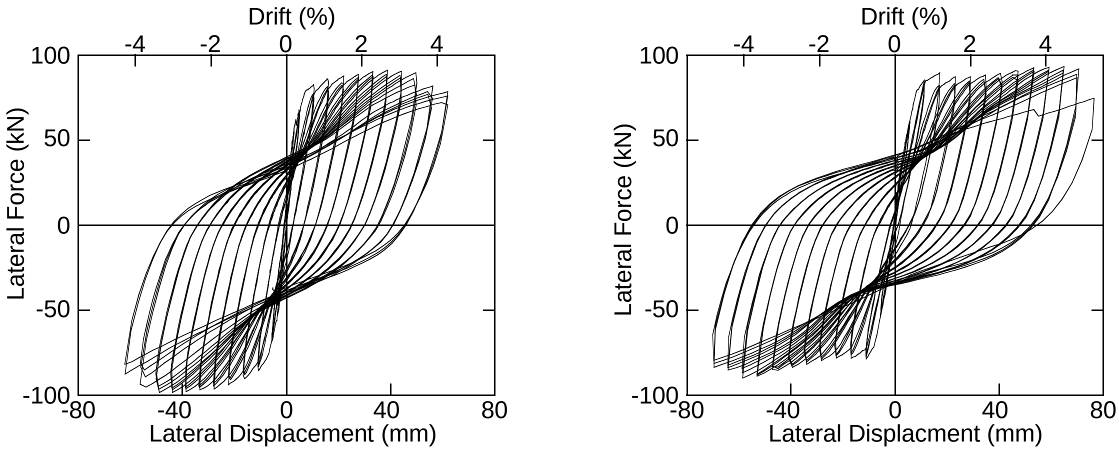


(1) Standard Column　　(2) Unbonded Column

Fig.4.52 Lateral Force vs. Lateral Displacement Hystereses

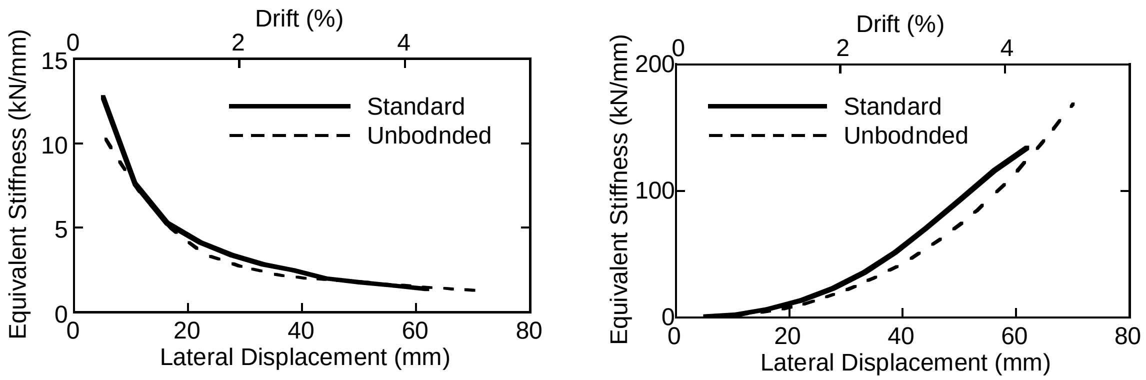


(1) Equivalent Lateral Stiffness　　(b) Accumulated Energy Dissipation

Fig.4.53 Equivalent Lateral Stiffness and Energy Dissipation

An important feature of the unbonded column is a rocking response of the column relative to the footing. Since the longitudinal bars are unbonded for a length of $L_{ub}$, the longitudinal bars in tension pull out from the column, which results in a dominant rocking response of the column. As a result of small flexural deformation, the flexural failure of the column is limited.

Fig. 4.52 compares the lateral force vs. lateral displacement hystereses. The restoring force of the standard column starts to deteriorate at $9\delta_y$ (=3.9% drift), while the restoring force is stable until $11\delta_y$ (=4.8% drift) in the unbonded column.

As a result of the deformation of the unbonded longitudinal bars in the plastic hinge, the initial lateral stiffness is slightly smaller in the unbonded column than the standard column. Fig. 4.53 compares the equivalent lateral stiffness and the accumulated energy dissipation between the unbonded and standard columns. The equivalent lateral stiffness is defined here as the secant stiffness between the maximum and minimum displacements in a hysteresis loop at each loading displacement. Although the equivalent lateral stiffness is slightly smaller in the unbonded column than the standard column when the lateral displacement is smaller than 1% drift, the difference between the two columns becomes small as the lateral displacement becomes large. This is due to the larger deterioration of the standard column. The difference of the accumulated energy dissipation between the two columns is negligible.

Although the longitudinal bars were unbonded in the plastic hinge of the column in the above examples, it is feasible to unbond the longitudinal bars in the footing or partly above and below the footing. Similar results were obtained by unbonding the longitudinal bars inside a footing [Hoshikuma, Unjoh, Nagaya 2000].

Based on the studies, it is considered that the unbonding is an effective means to increase the ductility capacity of columns by properly choosing the unbond length $L_{ub}$.

**3) Prestressed concrete columns**

It is well known that prestressed concrete members exhibit stable seismic performance under a combined action of shear and flexure. Consequently, it is anticipated that the flexure and the shear capacities can be enhanced in the prestressed concrete columns in comparison to the standard reinforced concrete columns. It is also anticipated that residual displacements after an extreme earthquake may be smaller in prestressed concrete columns than reinforced concrete columns. It may be possible to reduce construction periods by using precast concrete segments.

However, prestressed concrete columns have been seldom constructed throughout the world in spite of their merits. Lack of practice and possible cost increases may be the main reason for limiting the implementation of prestressed concrete columns. It is also sometimes pointed out that the energy dissipation is less in prestressed concrete columns than reinforced concrete columns because fewer concrete cracks dissipate less energy.

To verify the seismic performance of prestressed concrete columns, an extensive experimental and analytical study was conducted (Ikeda1998, Ikeda, Mori, Yoshioka 1998, Mutsuyoshi, Zatar, Maki 2001). In the loading test, rectangular prestressed concrete columns with an effective height of 1.5 m and a section of 400 mm by 400 mm were constructed. The concrete strength, the prestress and bond/unbond of the PC cables were studied as parameters.

Fig. 4.54 shows the effectiveness of the prestressed concrete columns in terms of the lateral force vs. lateral displacement hysteresis. The columns were subjected to an axial load (dead load of the superstructure) equivalent to 1MPa, and the prestress was either 4 or 8 MPa. They failed in flexure. The hysteresis of a standard reinforced concrete column is also presented here for comparison. A remarkable feature of the prestressed concrete columns is the rest-position oriented unloading hystereses. If one defines the unloaded residual displacement as a residual lateral displacement of a column when the lateral force is equal to zero after unloaded from a maximum lateral displacement, then the unloaded residual displacement is significantly smaller in the prestressed concrete columns than the standard reinforced concrete column. Fig. 4.55 shows how the unloaded residual displacement decreases as the prestress increases in the prestressed concrete columns. It is obvious from a nonlinear dynamic response analysis that the limited unloaded residual displacement contributes to reduce the residual displacement of a bridge after an extreme earthquake. This contributes to satisfy the requirement of Eq. (6/27).

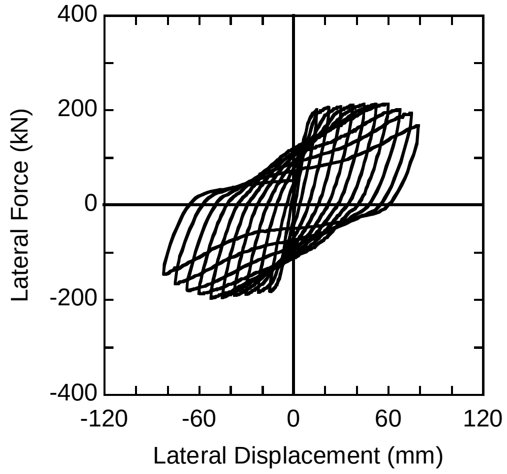


(a) Standard Column

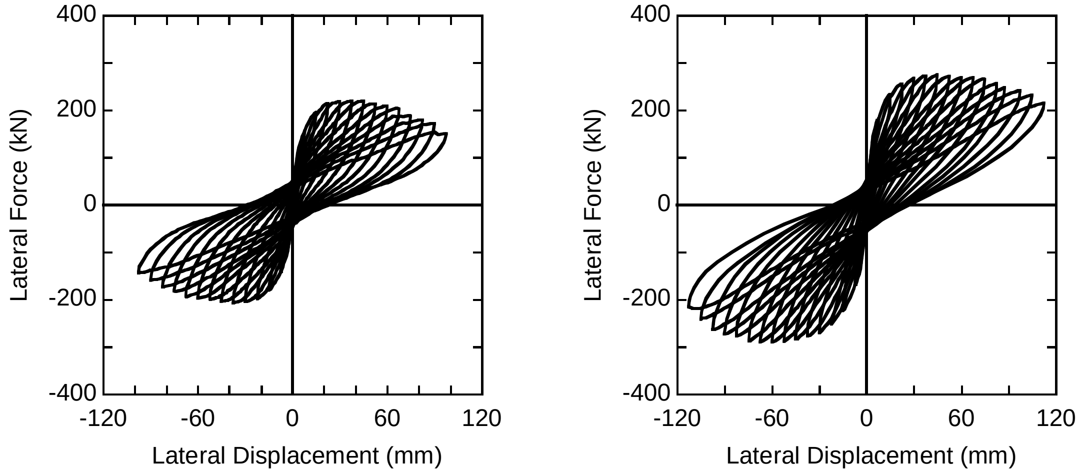


(b) Prestress=4Mpa (c) Prestress=8Mpa

Fig.4.54 Effect of Prestressing on the Hysteretic Behavior (Ikeda, Mori, Yoshioka 1998)

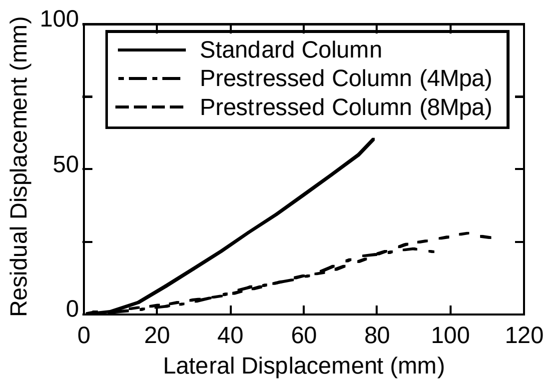


Fig. 4.55 Effect of Prestressing on the Unloaded Residual Displacement (Ikeda, Mori, Yoshioka 1998)

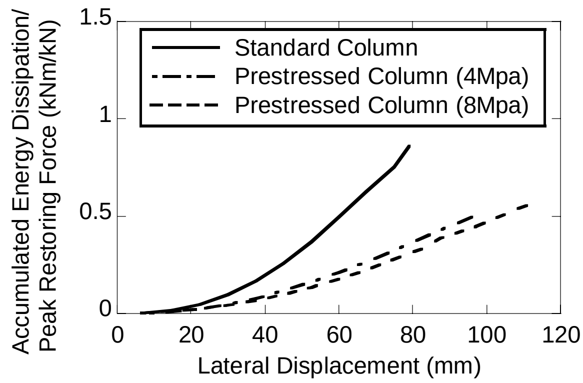


Fig. 4.56 Effect of Prestressing on Accumulated Energy Dissipation (Ikeda, Mori, Yoshioka 1998)

Number and size of concrete cracks were smaller in the prestressed columns than the standard reinforced concrete column during the loading and unloading reversals. The restoring force remarkably decreases when longitudinal bars locally buckle in the standard reinforced concrete, while such a remarkable deterioration of restoring force does not occur in the prestressed columns. Fig. 4.56 shows that the accumulated energy dissipations normalized by the peak restoring forces is smaller in the prestressed columns than the standard reinforced concrete columns as anticipated inherent to the rest-position oriented hysteretic behavior. This effect has to be considered in design based on the total response of a bridge system.

From the study, various merits of certain prestressed concrete columns were found. Those merits support the implementation of prestressed concrete columns.

**4) Isolator built-in column**

Since the hysteretic behavior of a reinforced concrete column occurs only at the plastic hinge, it is interesting to replace the concrete in the plastic hinge by an appropriate material that provides enough deformation and energy dissipation so that the flexural deformation in the rest of a column is limited. The material has to be sufficiently softer than the reinforced concrete column in order to reduce the flexural deformation of the column. By appropriately choosing the stiffness and strength of the material, it is expected that the reinforced concrete column with the material at the plastic hinge becomes free from damage under an extreme earthquake excitation. Several efforts have been already initiated for such a purpose. The major technical importance is what material should be used for the replacement of reinforced concrete at the plastic hinge. It must be sufficiently stable under repeated seismic loading with large strains, and durable for long term use. It is preferable if energy dissipation is available associated with the deformation of the material.

One material studied is a high damping rubber that is used for standard high damping rubber bearings for seismic isolation. The high damping rubber meets several of the requirements described above. It may be provided in the form of a rubber block or a laminated rubber. If one sets a high damping rubber unit at the bottom of a column, the column deforms as shown in Fig. 4.57 under a lateral seismic force. The longitudinal bars are continuous

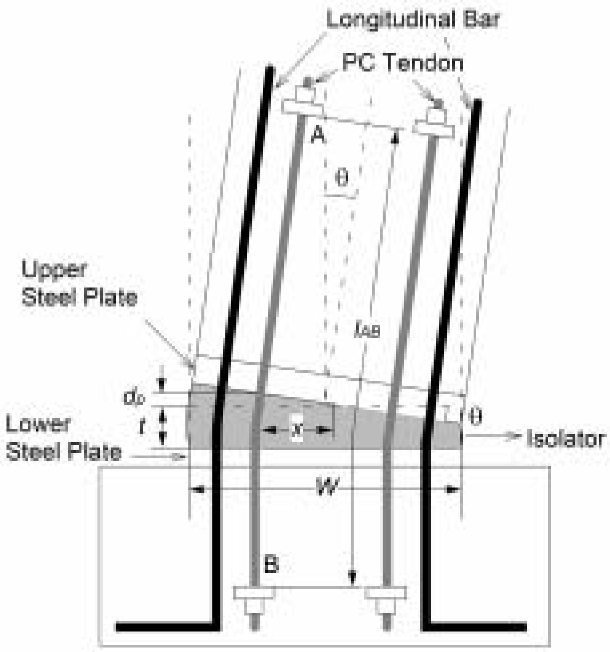


Fig.4.57 Isolator Built-in Column

through the rubber unit. Prestressed tendons may be effective to prevent sudden deterioration of restoring force and satisfy the requirement by Eq. (6.27) for the residual displacement.

The rubber unit does not resist tension if it is not anchored to the column and the footing. Since contact of the rubber unit with the column and the footing is limited if the rubber unit is not anchored to the column and the footing, slippage and rotation of the column relative to the footing occurs once the longitudinal bars yield under a cyclic lateral loading. Hence, the upper and lower steel plates which are galvanized to the rubber unit are anchored to the column and the footing by the anchor bolts. The longitudinal bars need to be continuous through holes in the steel plates and the rubber unit.

Laminated rubber units may be used if the rubber unit is thick. The steel plates in the laminated rubber unit may prevent the local buckling of the longitudinal bars when they are subjected to alternative tension and compression. Shear-keys may be required to prevent an excessive lateral displacement of the column relative to the footing when the rubber unit is thick.

Since such a column is nearly equivalent to a built-in high damping rubber isolator, it is called here an *isolator built-in column* (Kawashima, Nagai 2002).

A difficult barrier of the isolator built-in column is the deformation of the longitudinal bars. As a consequence of the column being supported by a flexible rubber unit, the longitudinal bars in the rubber unit are subjected to compression due to the self-weight of the structure. The longitudinal bars in the rubber unit are also subjected to repeated tension and compression with larger strain amplitude than a standard reinforced concrete column under an extreme earthquake excitation. Hence, it is likely that the longitudinal bars will locally buckle and rupture in the rubber unit. Consequently special attention has to be paid to prevent the premature failure of the longitudinal bars in the rubber unit. Use of special steels with the enhanced ductility may be effective.

If the stiffness of the rubber unit is sufficiently smaller than the stiffness of the column, major deformation under a lateral seismic force occurs in the rubber unit with the deformation of the column being limited. This results in the rocking response of the column similar to the unbonded column in 4.5 2). Representing the rotation of the column as $\theta$, the lateral displacement of the column at the top is $H \cdot \theta$ under the lateral force, in which $H$ represents the column height. Since the drift $d_r \approx H \cdot \theta / H = \theta$, if one expects to have stable response of the column until a drift of $d_r$, the strain at the compression fiber of the rubber unit $\varepsilon_r$ is

$$\varepsilon_r = \frac{\alpha W}{t}\theta \tag{4.77}$$

where $W$ is the column width, $t$ is the thickness of the rubber unit, and $\alpha$ is defined as $\alpha = x / W$ in which $x$ is the distance from the neutral axis to the compression fiber. Since the rubber unit shows the extensive strain hardening under high compression, its effect has to be included in the evaluation of stress $\sigma_r = f(\varepsilon_r)$ corresponding to the strain by Eq. (4.77). Deformation characteristics of rubber units under high compression as high as 120 MPa was studied to determine $f(\varepsilon_r)$. Consequently, the following relation has to be satisfied to avoid failure of concrete of the column

$$\sigma_r < \sigma_{cc} \tag{4.78}$$

where $\sigma_{cc}$ represents the concrete strength.

On the other hand, from Eq. (4.77), the rubber unit must be thicker than the following value so that it is stable under the repeated compression corresponding to the lateral drift $d_r$.

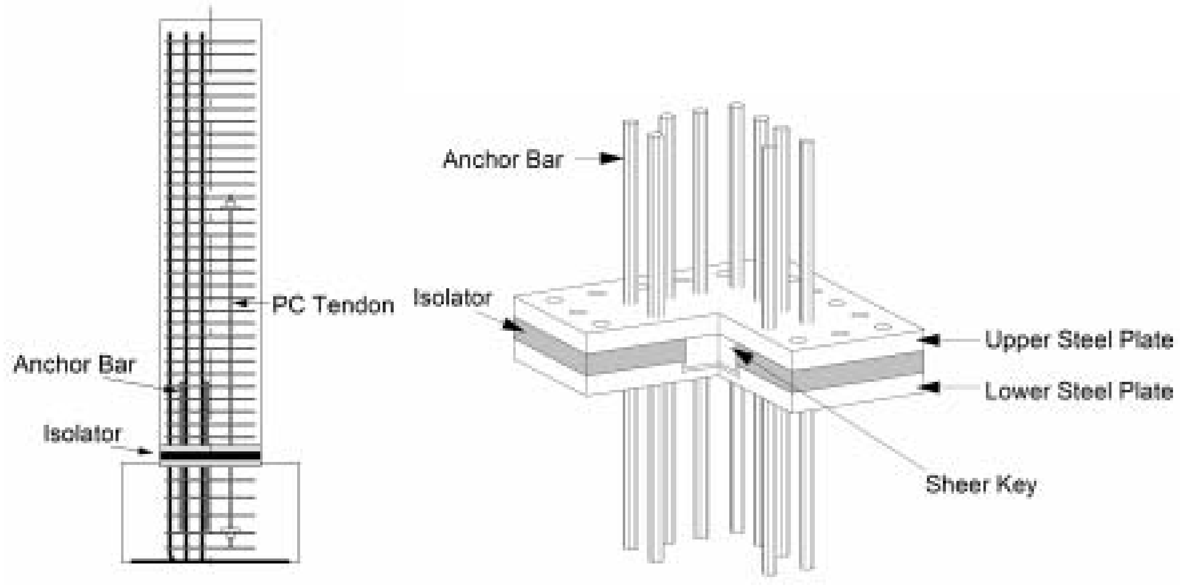


(a) Reinforcements (b) Rubber Unit with Anchor Bars

Fig.4.58 Model Columns

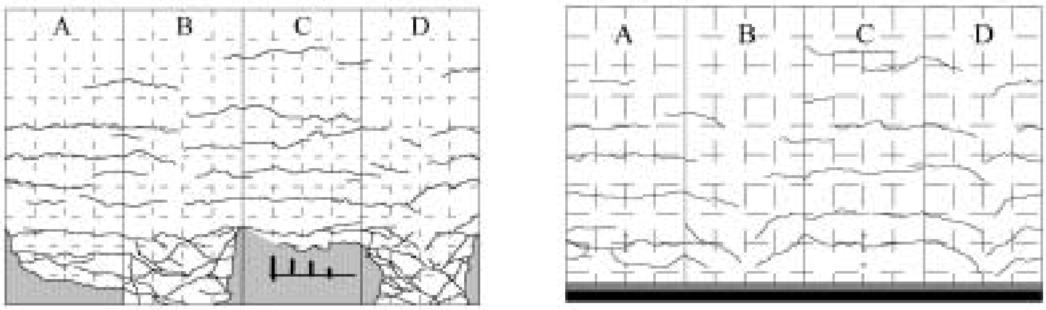


(a) Standard Column (b) Isolator Built-in Column

Fig.4.59 Failure of Columns after 4% Drift ( Loaded in AC Direction )

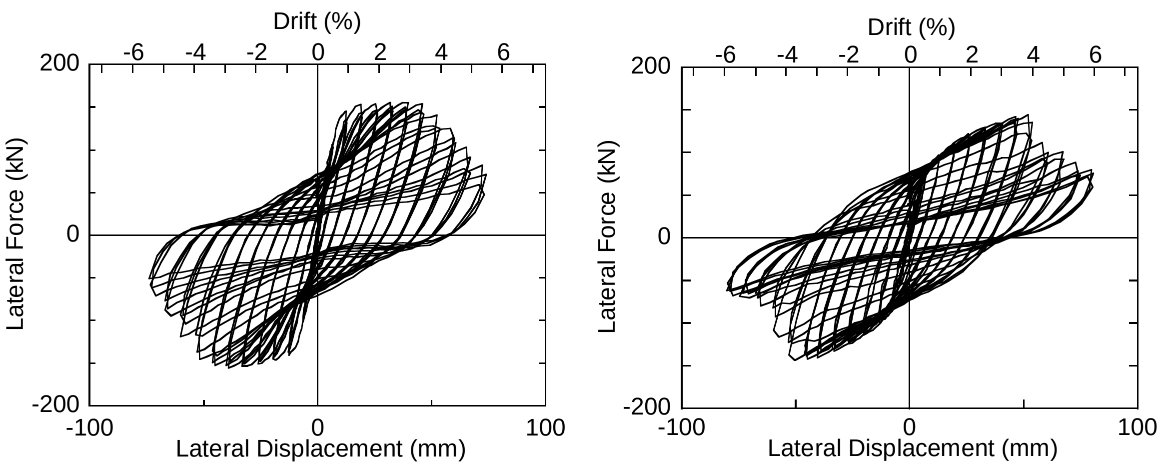


(a) Standard Column (b) Isolator Built-in Column

Fig.4.60 Lateral Force vs. Lateral Displacement Hystereses

$$t_{\min} > \frac{\alpha W}{\varepsilon_r} \cdot d_r \tag{4.79}$$

By designing the isolator built-in column based on Eqs. (4.78) and (4.79), the failure of concrete may be mitigated.

A series of seismic loading tests was conducted to verify the performance of the isolator built-in columns. Model columns were constructed 1350mm tall (effective height) with a 400mm by 400mm rectangular section as shown in Fig. 4.58. They were designed so that the hystereses are stable until 4% drift. As a consequence, 30 mm and 60 mm thick damping rubber units were used with an initial shear modulus of 1.2 MPa. Those rubber units are often used for seismic isolators for bridges. The longitudinal reinforcement ratio was 1.58%, and the volumetric tie reinforcement ratio was 0.79%. A shear-key was provided at the center, and four prestressed tendons were provided at the four corners.

Fig. 4.59 compares the failure of the isolator built-in column and the standard column after 4% drift loadings. Extensive failure of the concrete occurs until 4% drift at the compression fiber in the standard column. The longitudinal bars start to rupture at 5.5% drift, which results in the significant deterioration of restoring force. On the other hand, the failure of concrete is much limited in the isolator built-in column until 4% drift. However the longitudinal bars start to rupture in the rubber unit at 4.5% drift. The use of ductile steel is required to mitigate the rupture of the longitudinal bars as a result of concentration of strain at the bars in the rubber unit.

Fig. 4.60 compares the lateral force vs. lateral displacement relations of the two columns. A remarkable change of the shape of the hysteresis loops is seen. The lateral force is almost the constant in the post-yield zone in the standard column, while it increases as the lateral displacement increases in the isolator built-in column. The extensive deterioration of the restoring force at 4.5% drift results from the rupture of longitudinal bars in the isolator built-in column. An important difference of the isolator built-in column is the smaller initial stiffness, as shown in Fig. 4.61 (a), due to the soft deformation of the rubber unit. However, since the stiffness of the standard column deteriorates due to failure of the concrete, the lateral stiffness of the standard column becomes close to that of the isolator built-in column over 2.5% drift. The energy dissipation per load reversal is nearly the same between the isolator built-in column and the standard column as shown in Fig. 4.61 (b).

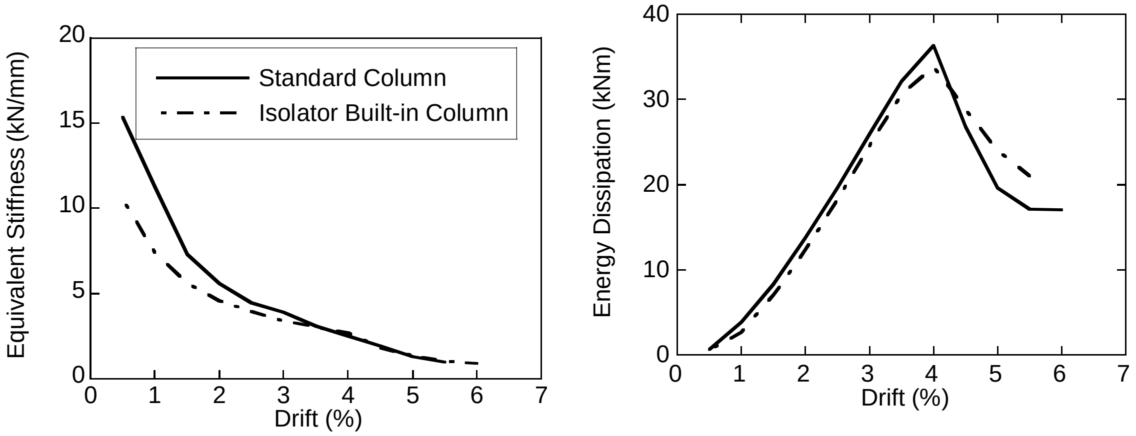


(a) Equivalent Stiffness (b) Energy Dissipation

Fig.4.61 Effect of Isolator on the Equivalent Stiffness and Energy Dissipation

### 4.6 Seismic Performance of C-Bent Columns

Although enhancing column ductility is important to assure the seismic performance of bridges under strong ground motions, a lower degree of static indeterminacy inherent to bridges is one of the most remarkable differences with buildings. There exist various unique structures which require special attention in the seismic design of bridges. One such structure is an inverted L-shape column, or C-bent column, with the lateral beam being longer on one side than the other side. An eccentricity $e$ between the column center and the point where the deck weight $D$ applies results in a static eccentric moment $D \cdot e$ in the column as shown in Fig. 17. This is likely to cause an extensive failure and develop a large residual displacement in the compression side of the column under a strong excitation.

The effect of eccentricity in the C-bent column was first included in the JRA seismic design in 1996. It considers the moment distribution, including the eccentric moment $D \cdot e$ presented in Fig. 4.62, in the evaluation of the yield displacement and the ultimate displacement. The lateral force capacity and the ductility factor of the column in the direction of eccentricity, $P_{ue}$ and $\mu_e$, are estimated as

$$P_{ue} = P_u - \frac{M_e}{H} \tag{4.80}$$

$$\mu_e = 1 + \frac{u_{ue} - u_{ye}}{\alpha(u_{ye} - u_{0e})} \tag{4.81}$$

where, $M_e = D \cdot e$ is the eccentric moment, $P_u$ is the lateral force capacity of a column without the eccentricity, $u_{ye}$ and $u_{ue}$ are the yield and ultimate displacements of the column, respectively (evaluated by the fiber element analysis assuming the moment distribution presented in Fig. 4.62), $u_{0e}$ is the static column displacement by the eccentric moment $M_e$, $H$ is the column height, and $\alpha$ is the safety factor. The safety factor $\alpha$ is a value between 3.0 and 1.2 depending on the importance of the bridge and the type of ground motion (pulsive or repetitive ground accelerations). In the direction perpendicular to the eccentricity (transverse direction), the effect of eccentricity is disregarded. Columns are designed independently in two lateral directions.

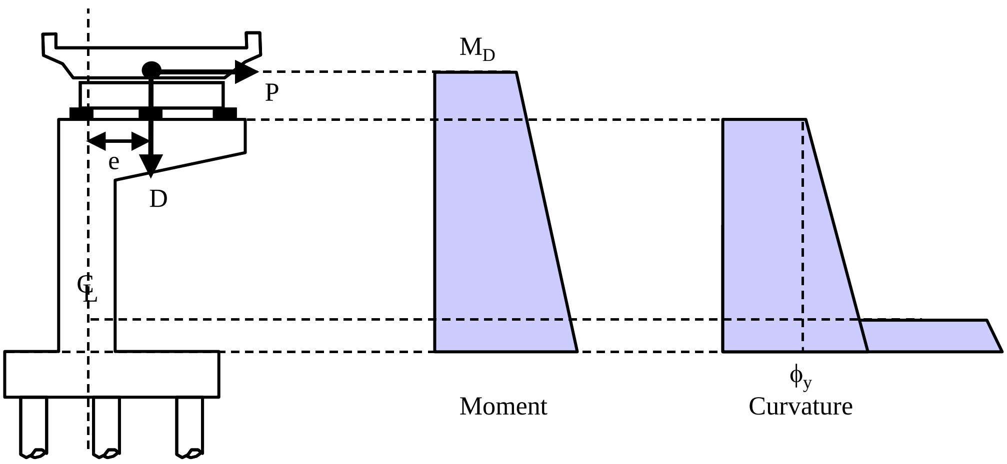


Fig. 4.62 Distribution for the Evaluation of Lateral Force and Ductility Capacities of a C-bent Column

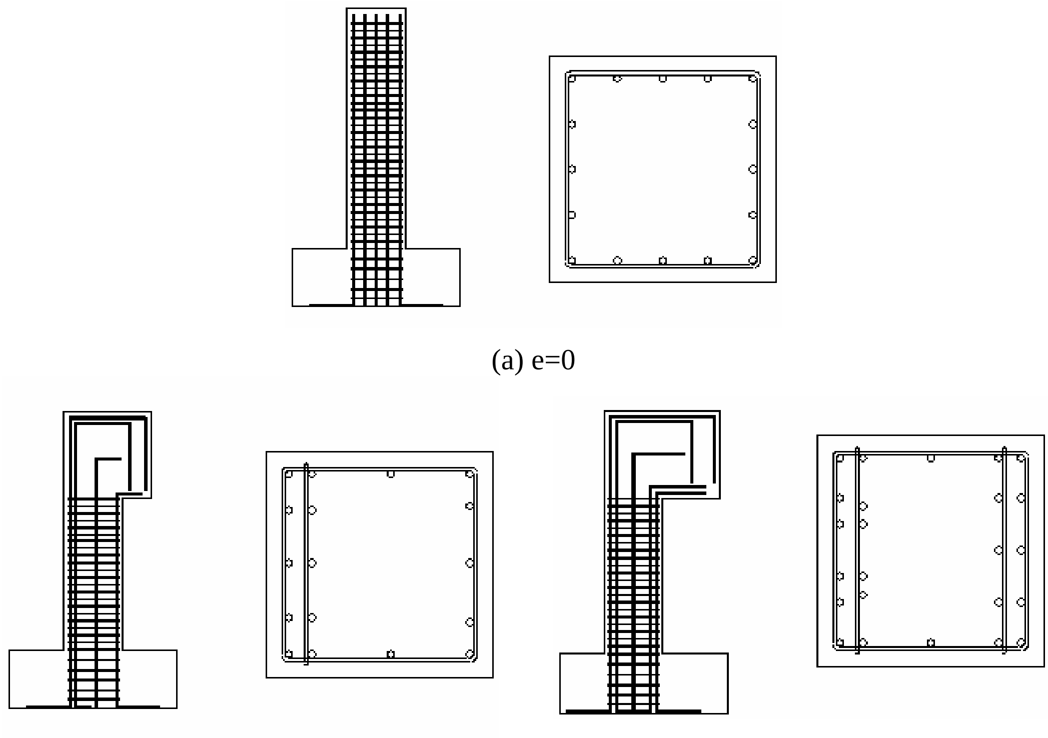

(a) e=0

(b) e=0.5D (c) e=1D

Fig.4.63 Reinforcement of C-Bent Column

The performance of C-bent columns was studied based on a cyclic loading test using columns with a rectangular section of 400 mm by 400 mm (Kawashima, Watanabe, Hatada 2002). The eccentricity $e$ was varied from 0, 0.5D and 1D, in which D is the column width. The columns were designed in accordance with Eqs. (4.80) and (4.81) to set the reinforcements as shown in Fig. 4.63. Longitudinal bars were provided in double at the side opposite from the eccentricity in the column when the eccentricity $e$ equals to 0.5D. When the eccentricity $e$ equals to D, longitudinal bars were provided in double not only on the side opposite from the eccentricity but also on the side of eccentricity in the column. The columns were loaded in the axial direction (direction perpendicular to the eccentricity), the transverse direction (direction parallel to the eccentricity), and bilateral directions under a constant vertical load. The column was loaded in a rectangular orbit as shown in Fig. 4.64 in the bilateral excitation.

Fig. 4.65 shows the progress of failure for the columns, with the eccentricity $e$=0 and 1D, under the bilateral directions. The failure mode is significantly different between the two specimens. The column with 1D eccentricity not only displaces laterally but also rotates around the column axis due to the eccentricity. As a result of rotation, the failure of concrete started at 2 corners in the eccentricity direction, and progressed to 4 surfaces. Extensive buckling and rupture of longitudinal bars occurred, and concrete spalled so that inner reinforcements are exposed at 3% drift. The column with 1D eccentricity deteriorates much faster than the column without eccentricity.

Another significant feature of the C-bent columns is the tilting of the columns in the transverse direction under the longitudinal loading. Since the compression failure of concrete and the longitudinal bars was more destructive in the eccentric compression side than the

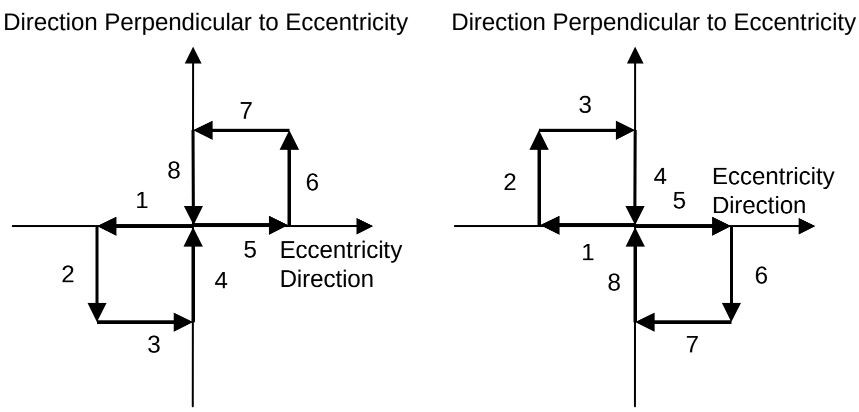


(a) drift 0.5%, 1.5%, … (b) drift 1.0%, 2.0%, …

Fig.4.64 Orbit of Bilateral Loading

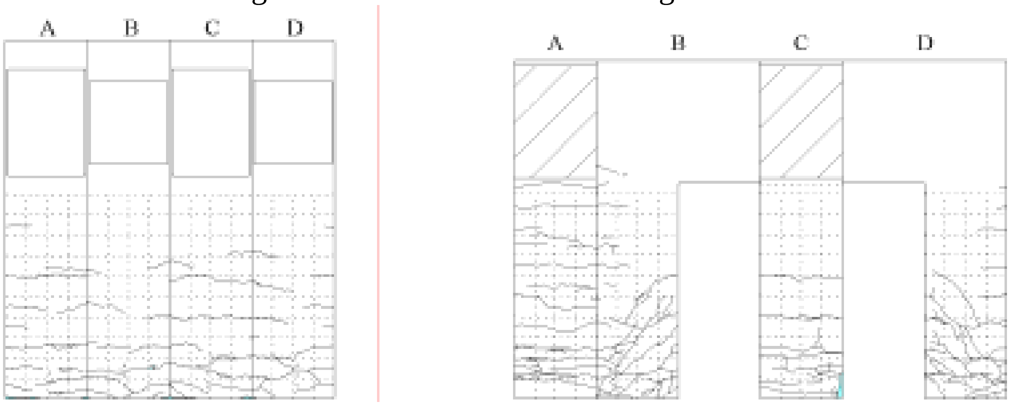


(a) Drift = 3% (b) Drift = 4%

(1) e=0

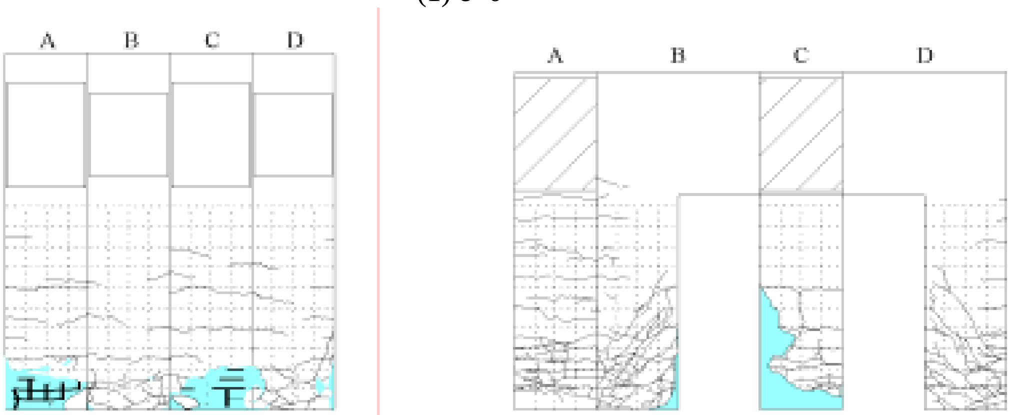


(a) Drift = 3% (b) Drift = 4%

(2) e=1D

Fig.4.65 Progress of Failure of the Inverted C-Bent column under Bilateral Loading

eccentric tension side, this resulted in the tilting of the column in the eccentricity compression direction. Fig. 4.66 shows the residual displacement of the columns with 0.5D and 1D eccentricities as a result of the tilting. The residual drift reaches 2.3% and 3.7% in the columns with the eccentricities of 0.5D and 1D, respectively, at 4% lateral drift. A similar experimental test was conducted by Tsuchiya et al [28].

Fig. 4.67 shows the lateral force vs. lateral displacement hystereses of the two specimens

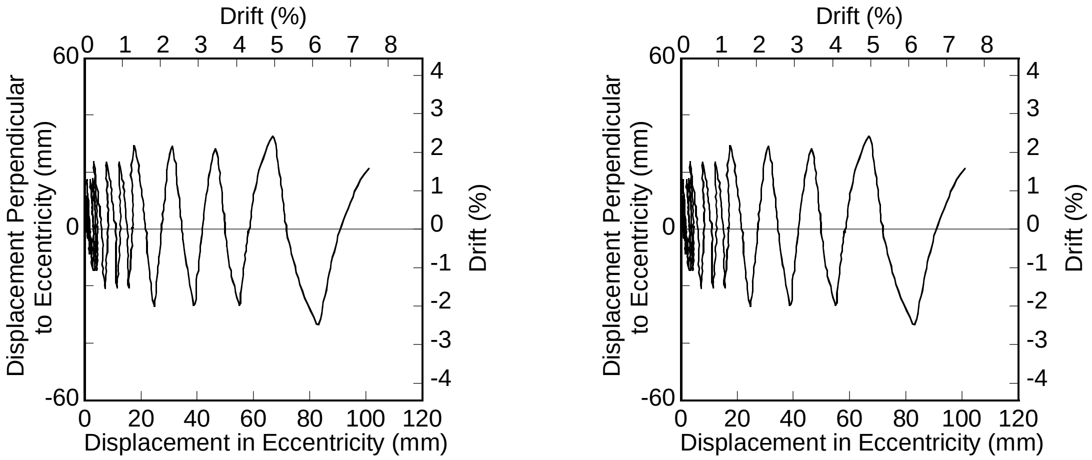


(a) e=0.5D (b) e=1D

Fig.4.66 Progress of Residual Displacement in the Direction of Eccentricity under a Cyclic Loading in the Direction Perpendicular to the Eccentricity

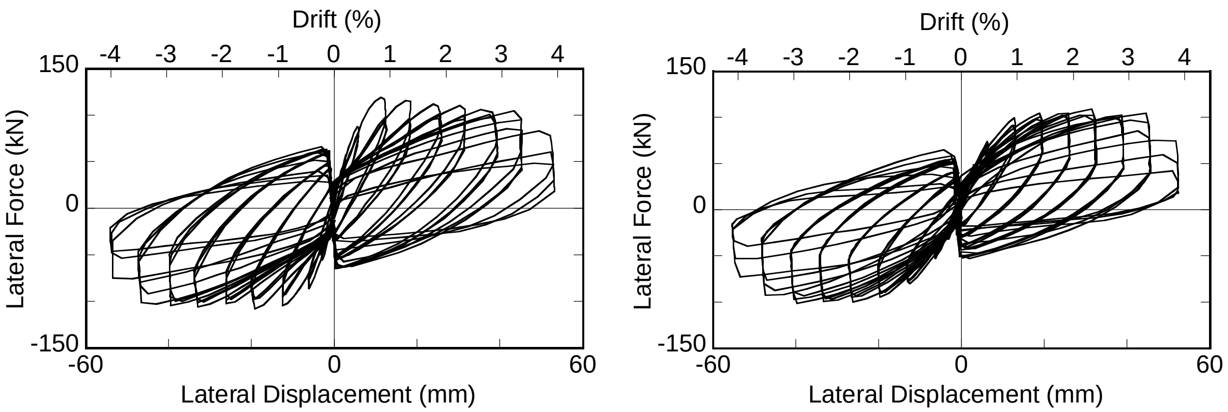


(a) Eccentricity Direction (b) Perpendicular to Eccentricity Direction

(1) e=0

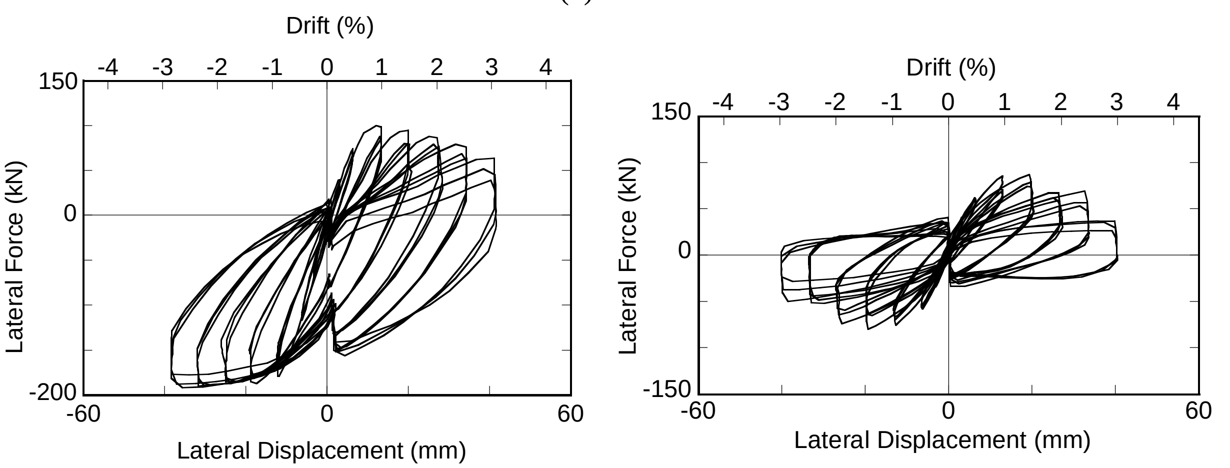


(a) Eccentricity Direction (b) Perpendicular to Eccentricity Direction

(2) e=D

Fig.4.67 Lateral Force vs. Lateral Displacement Hystereses under Bilateral Loading in two lateral directions. Since one actuator was held while the other actuator was loaded in the bilateral loading (refer to Fig. 4.64), the hysteresis is narrow at the small displacement. The hystereses are stable until 3.5% drift in both directions in the column without eccentricity, while the restoring force significantly deteriorates at 2.5% drift in the column with 1D eccentricity. It is noted that the deterioration of restoring force is significant in the direction perpendicular to the eccentricity (transverse direction).

Careful analyses are required for the columns with eccentricities to determine their restoring force and ductility capacities.

## REFERENCES


Applied Technical Council (1996), “Improved seismic design criteria for California bridges: Provisional recommendations,” ATC 32, Redwood, CA, USA.

Ban, S. and Muguruma, H. (1960), “Behavior of plain concrete under dynamic loading with straining rate comparable to earthquake loading,” 2nd World Conference on Earthquake Engineering, Vol. III, 1979-1993

California Department of Transportation (1999), “Bridge memo to designers, 20-1 Seismic design methodology,” Sacramento, CA, USA

Dott, L.L., and Cooke, N. (1992), “The dynamic behavior of reinforced concrete bridge piers subjected to New Zealand seismicity,” Report 92-4, Department of Civil Engineering, University of Canterbury, New Zealand

European Prestandard (1994), ”Eurocode 8 - Design provisions for earthquake resistance of structures,” Brussels

Federal Highway Administration (2002), “Guidelines for seismic performance testing of bridge piers (first draft),” Department of Transportation, USA

Fujikura, S., Kawashima, K., Shoji, G., Jiandong, Z. and Takemura, H. (2000), “Effect of the interlocking ties and cross ties on the dynamic strength and ductility of rectangular reinforced concrete bridge piers,” Structural and Earthquake Engineering, Proc. JSCE, 640/I-50, 71-88

Hoshikuma, J., Unjoh, S. and Nagaya, K., (2000), “Experimental study for the enhancement of seismic performance of reinforced concrete columns,” 1st Symposium for Enhancement of Seismic Disaster Prevention, JSCE, 135-140

Hoshikuma, J., Unjoh, S. and Nagaya, K., (2002), “Flexural ductility of full-scale bridge columns subjected to cyclic loading,” First fib Congress, Osaka, Japan

Hosotani, M, Kawashima, K. and Hoshikuma, J. (1998), “A stress-strain model for concrete cylinders confined by carbon fiber sheets,” Journal of Concrete Engineering, JSCE, 592/V-39, 37-53

Hosotani, M. and Kawashima, K. (1999), “A stress-strain model for concrete cylinders confined by both carbon fiber sheets and hop reinforcements,” Journal of Concrete Engineering, JSCE, 648/V-47, 137-154.

Hosotani, M., Kawashima, K. and Uji, K. (2000), “An evaluation model of ductility capacity of reinforced concrete bridge piers confined by carbon fiber sheets,” Journal of Concrete Engineering, JSCE, 592/V-39, 37-53

Ikeda, S. (1998), “Seismic behavior of reinforced concrete columns and improvement by vertical prestressing,” Proc. 13th FIP Congress on Challenges for Concrete in the Next Millennium, Vol. 2. pp. 879-884

Ikeda, S., Mori, T., and Yoshioka, T. (1998), “Seismic performance of prestressed concrete

columns," Prestressed Concrete, 40-5, 40-47
Iwata, S., Otaki, K. and Iemura, H. (2001), "Experimental study on the seismic retrofit and repair of large-scale reinforced concrete columns," 26th Earthquake Engineering Symposium, JSCE, 1393-1396
Japan Road Association (1996 and 2002), "Seismic design specifications of highway bridges," Maruzen, Tokyo, Japan
Kawashima, K. (2000), "Seismic performance of RC bridge piers in Japan: An evaluation after the 1995 Hyogo-ken nanbu earthquake," Progress in Structural Engineering and Materials, 2-1, pp. 82-91, John Wiley & Sons
Kawashima, K., Hosotani, M. and Yoneda, K. (2000), "Carbon fiber retrofit of reinforced concrete bridge piers," International Workshop on Annual Commemoration of Chi-Chi Earthquake, Vol. II-Technical Aspects, 124-135, National Center for Research on Earthquake Engineering, Taipei, Taiwan, R.O.C.
Kawashima, K., Hosoiri, K., Shoji, G. and Sakai, J. (2001), "Effects of unbonding of main reinforcements at plastic hinge region for enhanced ductility of reinforced concrete bridge columns," Structural and Earthquake Engineering, Proc. JSCE, 689/I-57, 45-64
Kawashima, K. and Nagai, M. (2002), "Development of a reinforced concrete pier with a rubber layer in the plastic hinge region," Structural and Earthquake Engineering, Proc. JSCE, 703/I-59, 113-128
Kawashima, K., Une, H. and Sakai, J. (2002), "Seismic performance of hollow reinforced concrete arch ribs subjected to cyclic lateral force under varying axial load," Journal of Structural Engineering, JSCE, 48A, 747-757
Kawashima, K., Watanabe, G., Hatada, S. and Hayakawa, R. (2002), "Seismic performance of C-bent columns based on a cyclic loading test," Proc. 3rd International Workshop on Performance-based Seismic Design and Retrofit of Transportation Facilities, Edited by Kawashima, K., Buckle, I. and Loh, C.H., TIT/EERG 02-2, 19-30, Tokyo Institute of Technology, Tokyo, Japan
Kent, D.C. and Park, R. (1971), "Flexural members with confined concrete," Journal of structural Division, ASCE, 97(7), 1969-1990
Mander, J., Priestley, N.M.J. and Park, R. (1986), "Theoretical stress-strain model for confined concrete," Journal of Structural Engineering, ASCE, 1114(8), 1804-1825.
Mander, J. B., Priestley, N.M.J. and Park, Ro. (1988), "Observed stress-strain behavior of confined concrete," Journal of Structural Engineering, ASCE, 114(8), 1827-1849
Menegotto, M. and Pinto, P.E. (1973), "Method of analysis for cyclically loaded RC plane frame including changes in geometry and non-elastic behavior of elements under combined normal force and bending moment," Proc. IABSE Symposium on Resistance and Ultimate Deformability of Structures Acted on by Well Defined Repeated Loads, 15-22
Mutsuyoshi, H., Zatar, W. A. and Maki, T. (2001), "Seismic behavior of partially prestressed concrete piers," Proc. JSCE, 669/V-50, 27-38
Park, R. (1996), "New Zealand perspectives on seismic design of bridges," Paper No. 2111 (CD-ROM), 11th World Conference on Earthquake engineering, Acapulco, Mexico, 1996
Priestley, N.M.J., Seible, F. and Calvi, M. (1996), "Seismic design and retrofit of bridges," John Wiley & Sons
Railway Technical Research Institute (1999), "Seismic design code for railway structures," Kokubunji, Japan
Roberts, J. (1999), "Optimizing post earthquake lifeline system reliability – seismic design details for bridges," Proc. 1st Workshop on Mitigation of Seismic Effects on Transportation Structures, Loh, C. H. et al editors, pp. 282-293, National Center for Research on Earthquake Engineering, Taipei, Taiwan, R.O.C.
Saaticioglu, M. and Razvi, S.R. (1972), "Strength and ductility of confined concrete," Journal

of Structural Engineering, ASCE, 118(6), 1590-1607
Sakai, J., Kawashima, K. and Shoji, G. (2000), “A stress-strain model for unloading and reloading of concrete confined by tie reinforcements,” Structural and Earthquake Engineering, Proc. JSCE, 654/I-52, 297-316
Sakai, J. and Kawashima, K. (2000), “Unloading and reloading stress-strain model for concrete confined by tie reinforcement,” Paper No. 1432 (CD-ROM), 12 World Conference on Earthquake Engineering, Auckland, New Zealand.
Sakai, J. and Kawashima, K. (2002), “Effect of varying axial loads including a constant tension on seismic performance of reinforced concrete bridge piers,” Journal of Structural Engineering, JSCE, 48A, 735-746
Shito,K. Igase,Y., Mizugami,Y., Ohasi,G., Miyagi,T. and Kuroiwa, T. (2002), “Seismic performance of bridge columns with interlocking spiral/hoop reinforcements,” First fib Congress, Osaka, Japan
Takiguchi, K., Okada, K. and Sakai, M. (1976), “Ductility capacity of bonded and unbonded reinforced concrete members,” Proc. Architectural Institute of Japan, 249, 1-11
Tanaka, H. and Park, R. (1999), “Seismic design and behavior of reinforced concrete columns with interlocking spirals,” ACI Structural Journal, 192-203
Tsuchiya, S., Ogasawara, M., Tsuno, K., Ichikawa, H., Maekawa, K. 1999), “Multi-axis flexure behavior and nonlinear analysis of RC columns subjected to eccentric axial forces,” Proc. JSCE, 634/V-45, 131-143
Yagishita, F., Tanaka, H. and Park, R. (1997), “Cyclic behavior of reinforced concrete columns with interlocking spirals,” Proc. JSCE, 19-2
Yen, P. (2002), “Guideline for testing method
Yoneda, K., Kawashima, K. and Shoji, G. (2001), “Seismic retrofit of circular reinforced concrete bridge columns by wrapping of carbon fiber sheets,” Journal of Structural Engineering and Earthquake Engineering, JSCE, 662/I-56, 41-56